Chapter

Solar-Driven Interfacial Evaporation: Advances and Opportunities

Yunqi Li, Haixiang Feng, Yu Qiu and Qing Li

Abstract

Solar-driven interfacial evaporation (SDIE) is a desalination technology based on interface heating and evaporation, which provides a potential strategy for developing green, environmentally protective, and economically efficient desalination. By now, the evaporation performances of solar-driven interfacial evaporation systems have been significantly improved due to the developments of photothermal materials and evaporator structures. Herein, the up-to-date approaches and results are summarized and elaborated on the mechanism of efficient photothermal conversion achieved by photothermal materials. The principle of enhancing the evaporation performance of SDIE systems has been systematically studied, and the existing feasible salt-resistant strategies for long-term desalination are summarized. Finally, the current challenges and outlooks of SDIE technology are discussed, providing a possible path for the development of this technology.

Keywords: solar-driven interfacial evaporation, photothermal conversion, evaporation performance, desalination, salt-resistant

1. Introduction

Water stands as the cornerstone of sustaining human life, fostering socio-economic progress, and enhancing material civilization. It intertwines deeply with diverse production endeavors and the day-to-day lives of individuals. Nevertheless, amidst the relentless economic expansion and burgeoning population, humanity's thirst for water resources continues to escalate. Compounding this challenge, environmental pollution and the unsustainable exploitation of water resources have culminated in water scarcity crises of varying intensities across numerous nations and regions, particularly in the Middle East and North Africa, where extreme water dearth is a perpetual reality [1]. For coastal metropolises and island nations, harnessing advanced desalination technologies to transform ocean waters into potable freshwater represents a viable solution to mitigate freshwater shortages [2]. However, conventional desalination methods, including reverse osmosis (RO) [3], multi-stage flash [4], and lectrodialysis [5], grapple with drawbacks like prodigious energy consumption, intricate and costly infrastructure requirements, and greenhouse gas (GHG) emissions, hindering their

widespread adoption in economically challenged regions. Hence, the urgent pursuit of novel desalination technologies that are cost-effective, energy-efficient, eco-friendly, sustainable, and highly productive holds paramount significance in reconciling the desalination-energy consumption paradox and alleviating the global freshwater crisis. By vigorously investing in such innovations, we can pave the way for a more secure and sustainable water future.

Solar energy, an abundant and pristine resource, has been harnessed since antiquity, contributing immensely to the advancement of human civilization. Photothermal conversion, a pivotal mode of harnessing this energy, not only provides the power for the natural processes of hydrological cycles and atmospheric circulation but also offers a beacon of hope in addressing water scarcity. Solar-driven evaporation, leveraging solar energy exclusively as its power source, circumvents the need for fossil fuels, thereby reconciling the conflict between freshwater availability and energy consumption. According to the position of photothermal materials in liquid media, the early solar-driven evaporation systems can be divided into two categories: bottom-heating system and bulk heating system (**Figure 1a** and **b**) [6]. The bottom-heating system is a solar-driven evaporation system in which sunlight usually needs to pass through the bulk water to be absorbed by the photothermal materials at the bottom surface (**Figure 1a**). This evaporation system requires heating the entire water body, resulting in significant heat loss, and its evaporation efficiency is only 30–45% [7]. The bulk heating system is a solar-driven evaporation system that directly absorbs and converts solar energy through nanoparticles dispersed in the fluids (**Figure 1b**) and can generate steam without heating the bulk water to boiling point. However, this system also faces the challenges of difficult pumping, easy aggregation, and deposition of nanofluids [8, 9].

In recent years, researchers have devoted significant efforts toward the development of advanced and highly efficient solar-driven evaporation systems, notably the interfacial heating system (depicted in **Figure 1c**). A pivotal moment occurred in 2014 when Prof. Chen's team at MIT and Prof. Deng's team from Shanghai Jiao Tong University concurrently published groundbreaking articles in Nature Communications [10] and Small [11], introducing the novel concept of interfacial evaporation at the air-water interface, respectively. The solar-driven interfacial

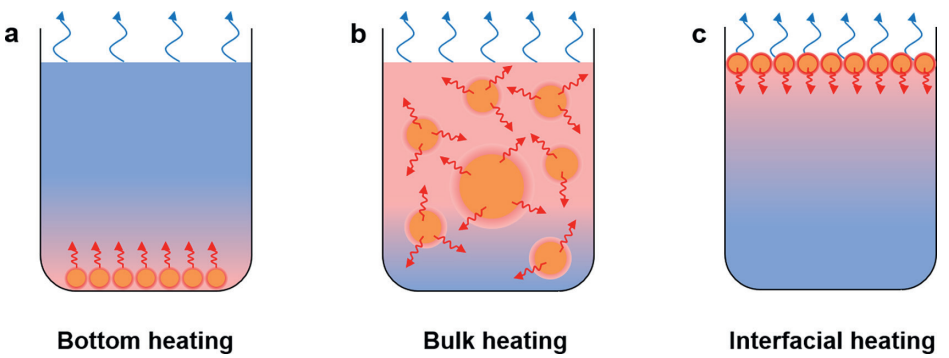

Figure 1.
Solar-driven evaporation through various forms of solar heating. (a) Bottom-heating system in which solar is absorbed by a solar absorber and converted into thermal energy to heat the bulk water from the bottom. (b) Bulk-heating system in which homogeneously dispersed solar absorbers (nanoparticles) convert incident solar photons into thermal energy to heat the bulk water. (c) Interfacial-heating system in which the solar-thermal conversion and evaporation are localized at the air-liquid interface.

evaporation (SDIE) system distinguishes itself from other solar-driven evaporation systems by precisely locating the conversion of solar energy into thermal energy at the air-liquid interface, only heating the water at the interface thereby reducing heat loss and achieving excellent evaporation performance and efficient photothermal conversion efficiency. Furthermore, the effective evaporation process inherent in SDIE systems keeps the surface temperature of the absorbing material relatively low, which in turn mitigates convective and radiative heat losses at the material's surface [6].

A conventional solar-driven interfacial evaporation system adopts a bilayer structure, as illustrated in **Figure 2**. The top layer comprises a solar-absorbing layer designed to efficiently capture and convert solar energy into heat, while simultaneously permitting the passage of steam through its surface without substantial contact with the underlying bulk water. The bottom layer serves a dual purpose: it restricts the conduction of heat generated by the photothermal materials into the bulk water, ensuring minimal heat loss, and provides mechanical stability and support for the solar-absorbing layer. Furthermore, this bottom layer necessitates a microporous structure featuring interconnected channels to efficiently supply water to the heated region, fostering rapid and stable evaporation rates.

In the past decade, this technology has experienced rapid development, with evaporation efficiency increasing to over 90% under conventional solar concentration, mainly enable by the continuous improvement and innovation of new photothermal materials and evaporator structural engineering [12–15]. The emergence of these new photothermal materials is mainly benefited from the continuous progress and development of modern nanotechnology in materials science. The vast majority of these photothermal materials has a light absorption rate of over 95% [16], which provides a guarantee for efficient solar-driven interface evaporation. Furthermore, a reasonable evaporator structure design has also made an important contribution to minimizing the system's heat loss. With the continuous development of solar-driven interfacial evaporation technology, it is possible to provide new insights for the application of the energy industry in modern society. Currently, solar-driven interface evaporation technology has achieved zero greenhouse gas emissions while providing clean water, making it an attractive advantage in addressing clean energy demand, water scarcity, and global warming issues.

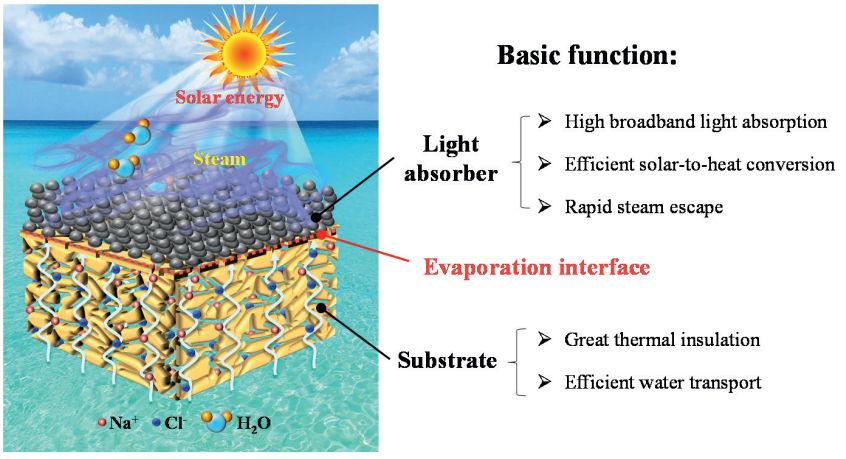

Figure 2.
The overall structural scheme of a typical bilayer interfacial solar-driven evaporation device.

This chapter provides a detailed introduction to the development of solar-driven interfacial evaporation technology, including the selection of various types of photothermal materials and supporting substrates and structural engineering strategies to improve thermal efficiency, and points out the opportunities and challenges faced by the further development of this technology.

2. Design principles to high evaporation performance

The evaporation performance of solar-driven interfacial evaporation systems is closely related to three factors, namely the solar absorption, thermal management and water transport [17]. It is worth noting that these three factors are closely related rather than independent of each other. The use of reasonable photothermal structure design to synergistically match these factors is intuitively important for optimizing the evaporation performance of the interfacial evaporation system. Therefore, this section first introduces the performance evaluation indicators of the interfacial evaporation system and then describes in detail three key strategies to improve evaporation performance: (i) efficient solar absorption; (ii) rapid and sufficient water transport; and (iii) excellent thermal management.

2.1 Evaluation indicators for evaporation performance

The performance of the solar-driven interfacial evaporation (SDIE) system is critically evaluated through two key indicators: evaporation rate and evaporation efficiency. The evaporation rate represents the mass variation of the SDIE system per unit time and unit area, which can be mathematically quantified using Eq. (1). In addition, evaporation efficiency measures the fraction of incoming solar flux that is effectively converted into stored thermal energy within the generated vapor, a calculation facilitated by Eq. (2). Both indicators provide valuable insights into the system's operational effectiveness and efficiency.

$$M = \frac{\Delta m}{S \cdot t} \tag{1}$$

$$\eta = \frac{M h_{eva}}{C_{opt} P_0} \tag{2}$$

where M refers to the evaporation rate of water, $\triangle m$ refers to the mass changes of the system, S is the projected area of the evaporator, t is the running time of the system, η refers to the evaporation efficiency, h_{eva} is the total liquid-vapor phase-change enthalpy (including the sensible heat), P_0 is the nominal solar irradiation value of 1 kW m^{-2}, and C_{opt} represents the optical concentration.

The theoretical limit of the evaporation rate of water under 1 kW m^{-2} illumination is 1.47 kg m^{-2} h^{-1} (3600 × 1 kW m^{-2}/2450 kJ kg^{-1} ≈ 1.47 kg m^{-2} h^{-1}). Nevertheless, numerous evaporator systems reported in literature exhibit evaporation rates surpassing this theoretical limit, leading to evaporation efficiencies that exceed 100% [18]. Consequently, when assessing the actual evaporation efficiency of a system, it is imperative to account for the environmental energy absorbed by the system and the variations in the enthalpy of water evaporation. Taking these factors into account, the precise evaporation efficiency of the system can be accurately calculated by

$$\eta' = \frac{(M - M_{\text{dark}})h_{act}}{C_{opt}P_0} \tag{3}$$

where M_{dark} refers to the evaporation rate of water in dark conditions and h_{act} is the verily liquid-vapor phase-change enthalpy.

2.2 Efficient solar absorption

In a solar-driven interfacial evaporation system, when sunlight illuminates on the photothermal materials, they are absorbed and converted into thermal energy, which is used to heat the water at the air-liquid interface, a process known as solar heat localization. Thus, photothermal materials with a wide spectrum of solar absorption and efficient conversion of solar energy into heat to drive water evaporation are the key factors in achieving efficient solar-driven interfacial evaporation [6]. So far, hundreds types of photothermal materials have been developed and explored, which can be classified into carbon-based materials, plasmonic particles, and semiconductor materials based on the differences in photothermal conversion mechanisms [19–22].

2.2.1 Carbon-based materials

Carbon based materials typically exhibit strong solar absorption abilities and can convert solar energy into thermal energy through lattice vibrations. As shown in **Figure 3a**, in carbon-based materials, loosely held electrons can be easily excited

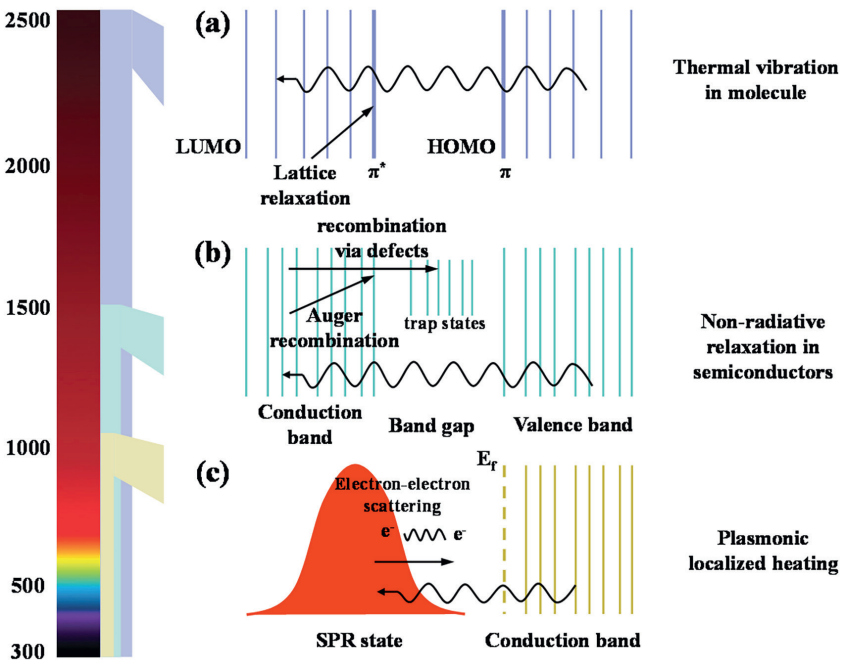

Figure 3.
The photothermal conversion mechanism and corresponding spectral absorption wavelength range of different types of photothermal materials. (a) Carbon-based materials. (b) Semiconductor materials. (c) Plasmonic particles.

from π orbitals to π* orbitals even with a small amount of energy input. When the photon energy of the incident light matches the possible electron transitions within the molecule, the excited electrons are lifted from the ground state (highest occupied molecular orbital, HOMO) to a higher energy orbital (lowest unoccupied molecular orbital), causing the excited electrons to relax back to the ground state and release heat [23, 24].

Because of their high solar absorption across a wide range of wavelengths (range from 250 nm to 2500 nm) and relatively low cost, carbon-based materials have been widely used in the field of solar-driven interfacial evaporation, such as graphene [25, 26], graphene oxide (GO) [27], reduced graphene oxide (rGO) [28], carbon nanotubes [29–31], and carbon black [32]. In addition, due to the strong stability and process-ability of carbon-based materials, they can be well integrated with porous substrates to enhance their solar absorption abilities and form stable evaporation structures.

2.2.2 Semiconductor materials

Recently, low-cost and low-toxicity semiconductors have emerged as a new type of photothermal material for solar-driven interfacial evaporation. Compared to carbon-based materials, there are fewer types of semiconductor materials, mainly metal oxide compounds, such as hydrogenated black titania [33], Fe_3O_4 [34], oxygen-deficient MoO_3 quantum dots [35], and bimetal oxides [36, 37]. As shown in **Figure 3b**, semiconductor materials have a high absorption for light in the wavelength range of 300–1500 nm [38]. In semiconductor materials, when the material absorbs light with energy similar to the bandgap, electron hole pairs are generated. In narrow bandgap semiconductors, due to the fact that the energy of most photons in the incident sun-light is higher than the energy of the bandgap, electron hole pairs above the bandgap will be generated. These electron hole pairs above the bandgap will then relax to the band edge, converting additional energy into heat through a thermalization process. In sharp contrast, when electron hole pairs recombine near the bandgap edge, most of the absorbed light energy is re-emitted in the form of photons in the wide bandgap semiconductor, resulting in much lower photothermal conversion efficiency [39].

2.2.3 Plasmonic particles

Plasmonic particle absorbers refer to various metal nanoparticles, such as gold (Au) [40, 41], silver (Ag) [41, 42], germanium (Ge) [43], and Au-Ag bimetals [41], etc., which have high solar absorption for light with wavelengths ranging from 300 nm to 1100 nm (**Figure 3c**) [44]. The photothermal conversion of the plasmonic particles is caused by the localized surface plasmon resonance (LSPR) effect of metals [45]. LSPR is a resonant photon-induced charge coherent oscillation that occurs when the photon frequency matches the natural frequency of the metal surface electrons. When sunlight shines on the surface of plasma, it excites electrons from occupied to unoccupied states, forming hot electrons (phonons) and redistributing energy through electron and electron-phonon scattering, causing the local surface temperature of the metal to rapidly rise. Then, the lattice cools through coupling and dissipates heat to the surrounding fluid.

In the early stage of research, to explore the solar evaporation performance using plasma nanoparticles, a self-assembly Au nanoparticles thin film with wide solar absorption spectrum was fabricated and placed at the air-liquid interface [46]. There is a significant heat loss from Au NP film to the bulk water because of their

direct contact. The photothermal conversion efficiency of the film system is only about 44%, but this is still more than twice as high as the efficiency of the gold NPs suspension system. To further improve the efficiency of photothermal conversion, plasmonic particle absorbers were deposited on the porous substrates (such as rough paper [19], wood [47–50], and multi-channeled anodic aluminum oxide (AAO) structure [51]) to reduce the heat loss of system. Due to the complex micro-interface morphology of porous substrates, multiple reflections and refractions of sunlight have been achieved, resulting in an ultra-high solar absorption of approximately 99% for plasmonic particle absorbers [41, 42].

2.3 Continuous and efficient water transport

Maintaining sufficient and continuous water supply through excellent water pathway design is the fundamental guarantee for achieving efficient and sustainable solar evaporation. In conventional solar evaporators, porous substrates typically have 3D random and interconnected porous structures that can continuously transport water from the underlaying water to the evaporation interface (**Figure 4a**). For example, it is by using natural porous materials [55–57] or commercial porous sponges [58] with rich internal porous structures as substrates to ensure sufficient water supply, and the interfacial evaporation system can be prepared by surface carbonization or loading photothermal materials. However, the thermal conductivity of these substrate materials increases after wetting, which leads to an increase in thermal loss from the evaporation interface to the bulk water, thereby weakening the thermal localization ability of the system.

To alleviate the problem of excessive thermal conductivity loss, a two-dimensional water pathway structure (**Figure 4b**) is formed by wrapping the water transport material on the surface of an insulation material with low thermal conductivity [47]. The evaporation system with this two-dimensional water pathway physically isolates the absorber from the bulk water through insulation materials, greatly suppressing parasitic heat loss. Compared with the overall water supply in conventional designs, the limited two-dimensional water channel structure reduces the dimensionality and volume of the water pathway, thereby minimizing the heat dissipation of the evaporation system to the bulk water [55]. Furthermore, as shown in **Figure 4c**, the dimension of the water pathway structure is reduced from 2D to 1D, forming a transport mechanism similar to water being transported from the mushroom stem to the cap [55]. And the water can be directly transported to the photothermal material through the

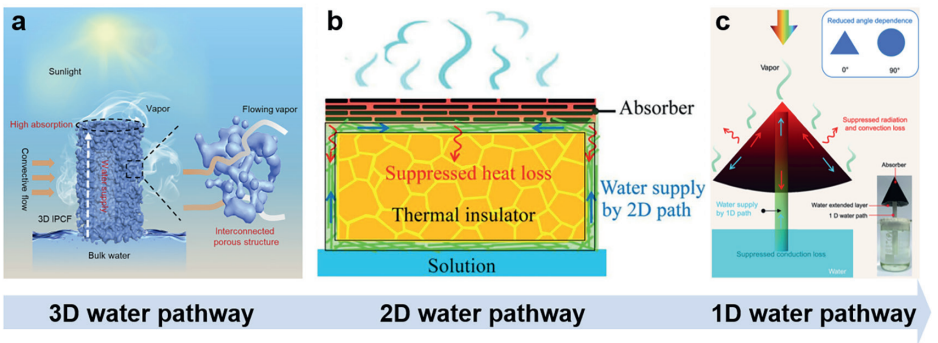

Figure 4.
The three types of evaporators with different water transport paths [52–54].

artificial core. In this 1D water pathway, the downward heat loss is perfectly minimized due to negligible contact with the bulk water.

2.4 Excellent thermal management

In the evaporation system with different water pathway, water transport and heat transfer are closely related. If water transport is too fast, it will increase the system's heat loss. Therefore, reasonable thermal management is also crucial to improve system performance.

After the photothermal material at the interface absorbs sunlight and converts it into thermal energy, it is necessary to ensure that the heat is effectively absorbed by the water at the interface and avoid significant heat loss as much as possible. **Figure 5** illustrates the heat transfer process in a solar-driven interface evaporation system. After the solar energy is absorbed and converted into heat, the vast majority of heat is absorbed by water to produce steam, and the remaining heat is consumed through convection, heat conduction, and radiation.

$$\alpha q_{\text{solar}} = q_{\text{evap}} + q_{\text{conv},air} + q_{rad,air} + \left(q_{\text{cond,water}} + q_{rad,\text{water}}\right) \tag{4}$$

where α is the solar absorption, q_{solar} refers to the solar flux, q_{evap} is the energy used for water evaporation, $q_{\text{conv,air}}$ and $q_{\text{rad,air}}$ are the radiative heat loss and convective heat loss at the evaporation interface, and $q_{\text{cond,water}}$ and $q_{\text{rad,water}}$ are the radiative heat loss and conduction heat loss from the evaporation interface to bulk water.

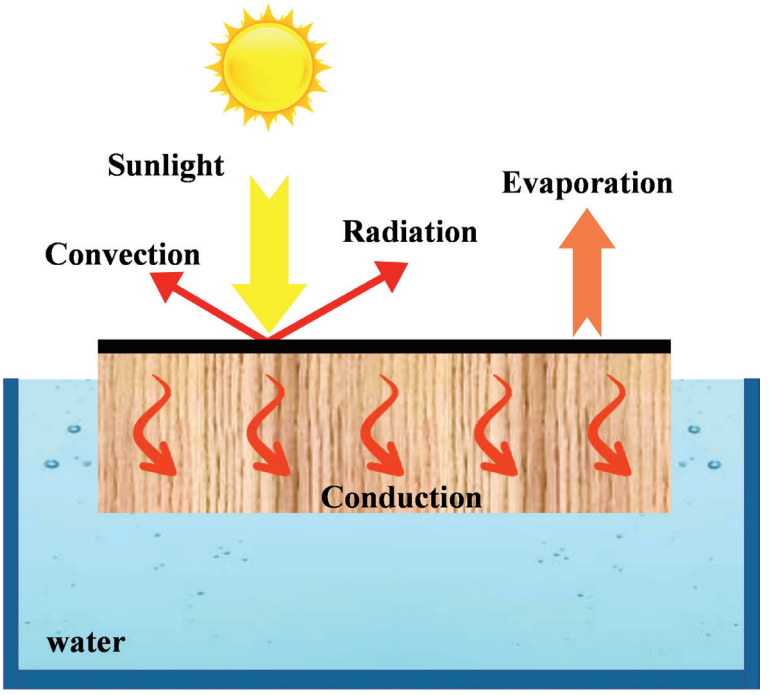

Figure 5.
The heat transfer process within a solar evaporator.

Generally, the heat loss transferred from the evaporator surface to the bulk water accounts for the largest proportion of the total heat loss [18]. The three types water pathways shown in **Figure 4** correspond to the three thermal management methods. For the evaporation system with 3D water pathway, the water is transported to the evaporation interface through the water transport paths. When the water transport layer is submerged in water, its overall wet thermal conductivity significantly increases due to the high thermal conductivity of water (approximately 0.60 $W{\cdot}m^{-1}{\cdot}K^{-1}$, 20 °C), resulting in increased heat loss. Therefore, it is necessary to choose materials with lower wet thermal conductivity to prepare the evaporators. Fortunately, many natural materials in nature have 3D water pathways and still have good thermal insulation properties after immersion. By carbonizing or adding coatings to these materials, high-performance evaporators can be made. Evaporation systems with 2D water pathways often use hydrophilic materials to transport water, avoiding extensive contact between the evaporator and the bulk water, thereby reducing heat loss. Materials commonly used as hydrophilic materials include cellulose, silk fabrics, and air-laid paper, etc. For the evaporation systems with 1D water pathways, the contact between the absorption layer and the water transport channel can be ignored, and the downward heat loss is greatly reduced, thus greatly improving the evaporation performance of the system.

Although the reduction of water pathway dimensions helps to reduce system heat loss and achieve higher evaporation efficiency, the limited water convention between the evaporation system and bulk water will possibly pose a risk of salt accumulation, especially in seawater desalination, which is one of the major challenges faced by this technology.

3. Salt-resistant strategies

Although significant progress has been made in improving evaporation efficiency through the development of various new materials or structures, there is still a big gap from practical applications, and one of the main problems is salt precipitation on the surface of the evaporator. When dealing with the seawater, non-volatile salts, like NaCl, will precipitate on the evaporator, consequently decreasing the solar absorption, blocking the water transport, and reducing the evaporation rate. Even the evaporator stops working when the salt is severely accumulated [59]. Thus, the long-term stability of the evaporator depends on its salt resistance. Recently, some delicate and effective salt-resistance strategies have been put forward and developed, which significantly enhance the salt resistance and stability of the evaporator.

Timely removal of the precipitating salt is a universal method for stable operation. It means regularly peeling off or washing the salt crystals on the evaporator to keep the evaporator clean and maintain the evaporation performance [60]. This method is general and valid, but additional operations for salt removal may increase the running cost, and this will interrupt continuous production, resulting in increased operating costs and decreased productivity [61].

To avoid the transfer of salt to the evaporation interface, inspired by the antifouling property of the water lily, hydrophobicity has been effectively utilized to promote the salt resistance of the evaporators [62]. The hydrophobic evaporator can block water and salt ions away from the evaporator, thus eliminating the salt precipitation. Furthermore, the Janus evaporator with the hydrophobic top layer and the hydrophilic bottom layer is designed and fabricated to enhance the evaporation rate and salt resistance (**Figure 6**). The accumulated salt ions are repelled at the interface between

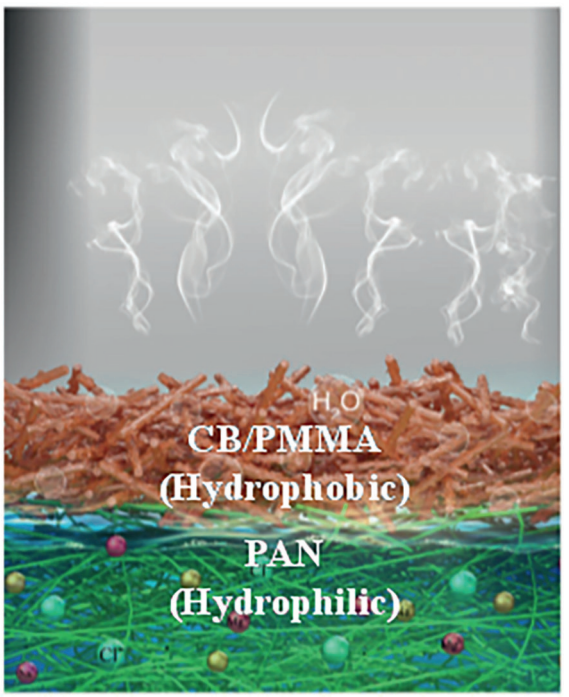

Figure 6.
Janus structure for enhancing salt resistance [63].

the hydrophobic and the hydrophilic layer, and they can timely diffuse back to the brine through the hydrophilic bottom layer, with a higher evaporation rate than the all-hydrophobic evaporator [63, 64].

During water transport, salt ions are always carried and raised to the evaporation region, which is the prerequisite for salt precipitation. Thus, separating water and salt ions during water transport is an imaginative method for enhancing salt resistance. Donnan effect can be utilized to repel the anion/cation from the charged hydrogel evaporator during the transport (**Figure 7**). Because the water supply layer of some hydrogel evaporators has a fixed charge, the co-ions are almost kept away from the

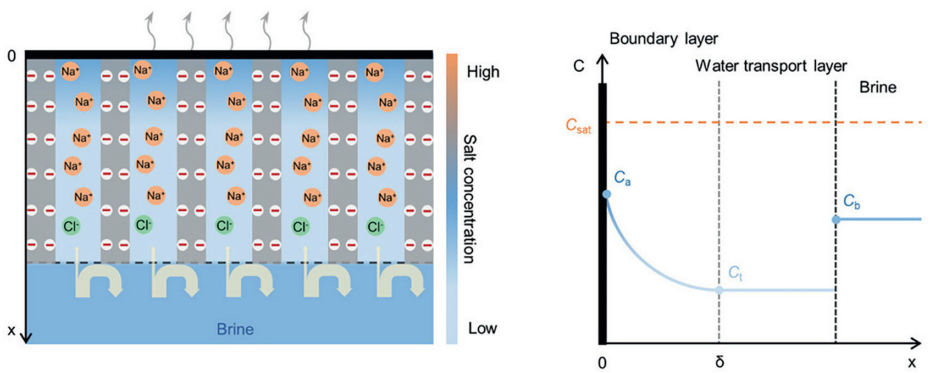

Figure 7.
Donnan effect for separating ions and water [65].

evaporator, and the counter-ions that enter the hydrogel with water are absorbed by the charged hydrogel due to electric neutrality, consequently separating the anion and cation and avoiding salt precipitation [65].

Actually, it is well recognized that the simplest and the most feasible method for salt resistance is to enhance the diffusion and convection of ions by accelerating the water transport. Because of the differences in the salt concentration and density between the evaporator and the bulk water, salt ions will flow back to the bulk water due to diffusion and convection. For example, some evaporators can dissolve the salt crystals when they do not work at night [66]. Therefore, speeding up diffusion and convection is an effective way to block salts (**Figure 8**). Normally, improving water transport can promote this process. For example, enhancing the hydrophilicity and designing additional water transport channels can improve the water supply, and the evaporators can stably work even under focus radiation and high salinity brine [67, 68]. Besides, according to the Fick's law, a short mass-transfer distance also causes a quick salt ion migration. Thus, reducing the tortuosity of the porous substance can shorten the distance of the ion migration and enhance the diffusion, consequently improving the salt resistance [69]. However, this method always promotes heat loss and reduces the evaporation rate because of the coupling between heat and mass transfer.

Besides the capillary force, incorporating other forces can further improve the water supply. For example, the Marangoni flow driven by differences in surface tension can quickly transport salt ions to the bulk water (**Figure 9a**) [70]. Moreover, the evaporator with a liquid level difference can form a directional flow to bring the ions away from the evaporation regions (**Figure 9b**) [71]. Besides, external electrical force and imbalanced torque are also utilized to migrate the ions and enhance the salt resistance [72, 73].

Except for the above strategies, contactless evaporation is a general and elaborate method for permanently blocking salt precipitation (**Figure 10**) [74]. The pivotal component of this method is an absorber/emitter unit above the water, which can convert the solar flux to mid-infrared radiation. Meanwhile, a thin water layer serving as the evaporator can efficiently absorb the mid-infrared radiation and evaporate (most within 100 μm layer). Thus, the solar absorber is completely and physically separated from the evaporator, and thus no salt will precipitate on this solar absorber. But this method always has a lower evaporation rate.

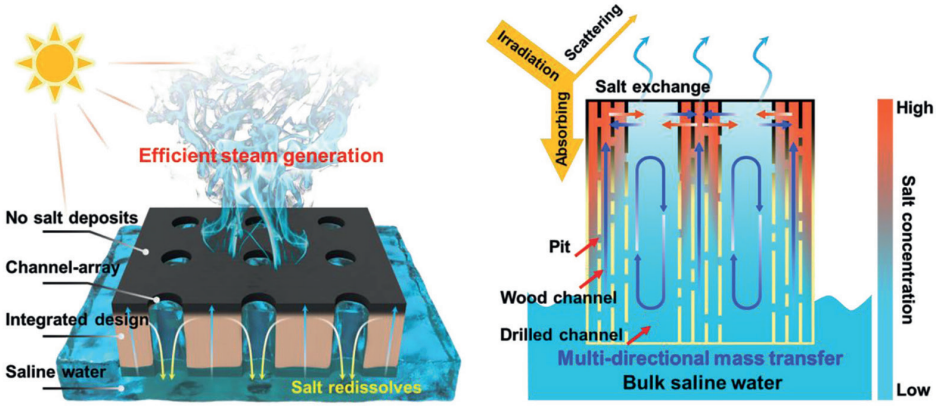

Figure 8.
Improved water supply for enhancing salt exchange and salt resistance [67].

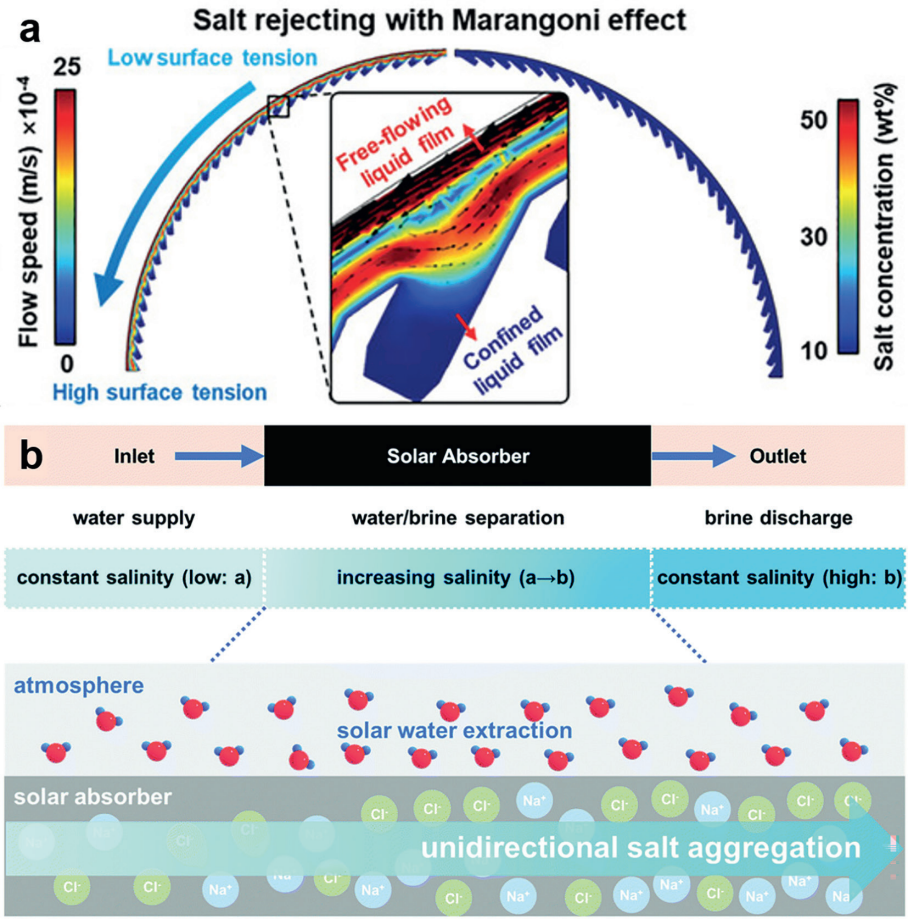

Figure 9.
Incorporating Marangoni effect [70] (a) and one-way flow [71] (b) for rapid salt ion migration.

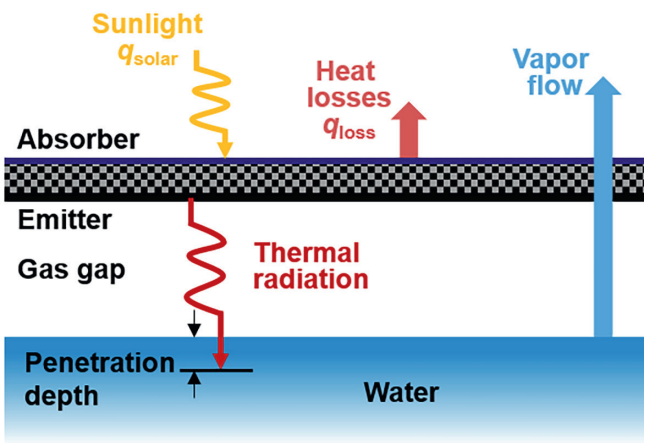

Figure 10.
The mechanism of the contactless evaporator [75].

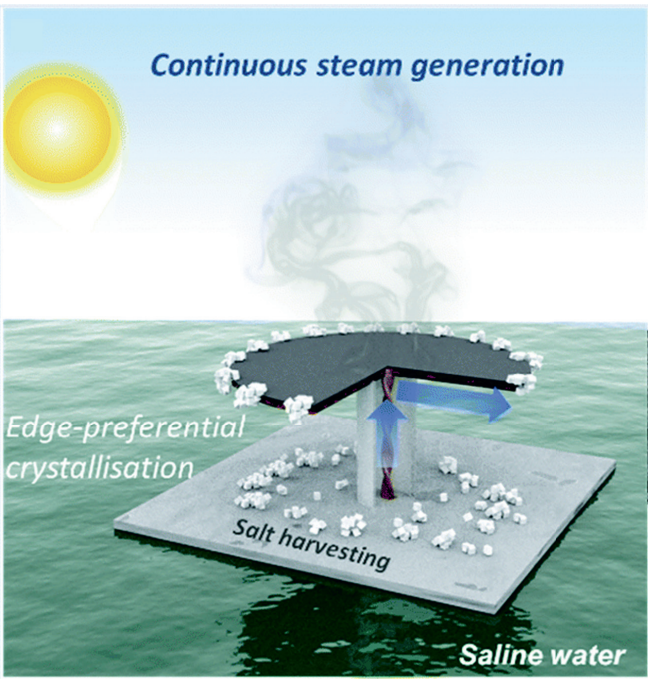

Figure 11.
One-way water transport channel for ZLD [76].

The above strategies can significantly enhance the salt resistance, but the salts always flow back to the brine, which causes the increasing salinity of the brine and is not beneficial for mineral recycle. Zero liquid discharge (ZLD) has been recognized as an efficient strategy to simultaneously harvest freshwater and salts even in high-salinity brine [76]. By purposively depositing the salt crystals on the edge of the evaporator and separating the photothermal surface from the salt deposit region, the evaporator can work steadily and recycle salts. For example, the evaporator with an ingenious one-way water transport channel from the central to the edge of the evaporator achieves a radially reduced water supply (**Figure 11**). Thus, the salt concentration increases from the central to the edge, and the salt crystals finally form at the edge of the evaporator, which does not affect the evaporation. Moreover, the salt crystals precipitating on the pre-wetted evaporator prefer to automatically be dropped by gravity force, consequently finishing the salt recycle. Thus, this method shows potential for water and mineral harvest and extends the application of SDIE.

In general, many efficient and ingenious salt-resistant methods have been proposed, and the salt resistance of the evaporator has been remarkably enhanced. Based on these methods, the evaporators can stably and continuously evaporate even under high-salinity brine. Thus, this technology shows potential for industrial desalination and stable access to fresh water.

4. Conclusions and outlooks

Solar-driven interfacial evaporation shows green, sustainable, and efficient character, which is a promising solution for alleviating the freshwater crisis. Owing

to the researchers' unremitting endeavor, the past decade has witnessed the rapid and remarkable development in the field of the solar-driven interfacial evaporation, which significantly enhances the evaporation rate and the salt resistance of the evaporator. Besides, it also can be utilized in the fields of electrical generation, wastewater purification, and fuel generation, indicating its extensive application. However, there are also some key issues limiting the scalable and commercial application, summarized as follows:

1. Deeper comprehension in the field of evaporation process. Though the evaporation rate has been remarkably enhanced, the understanding of this multi-field coupling evaporation process is limited. For example, the reason for the reduced evaporation enthalpy is not clear, and the energy transfer and conversion in the multifunction system are not revealed. Deep comprehension of SDIE is conducive to designing the evaporator with better performance. With the help of kinds of numerical simulations, the mechanism behind the evaporation may be uncovered.

2. Long-term stability. Due to the complexity of the actual seawater, it is necessary to consider the potential failure of the evaporator caused by kinds of organics, microorganisms, and salts. Thus, reasonable design for the evaporator with high resistance to contamination can efficiently prolong the longevity of the system and lower the cost.

3. Limited condensate collection. The evaporation rate in the open system has been remarkably enhanced, even breaking the theory limit. After integrating a transparent cover, this closed system can obtain freshwater. Different from the open system, the vapor will condense on the cover, which causes high optical loss. Then, limited condensation makes the humidity in the closed system quite high, consequently decreasing the evaporation. Eventually, the collection rate in the closed system is quite low, which is not beneficial for obtaining freshwater. Therefore, improving the collection rate by reasonable design is more meaningful for application.

In brief, it is necessary to deeply investigate the solar-driven interfacial evaporation, and this innovative and sustainable technology can play a more important role in efficiently obtaining freshwater.

Solar-Driven Interfacial Evaporation: Advances and Opportunities
DOI: http://dx.doi.org/10.5772/intechopen.1008570

Author details

Yunqi Li†, Haixiang Feng†, Yu Qiu and Qing Li*
School of Energy Science and Engineering, Central South University, Changsha, Hunan, China

*Address all correspondence to: qingli@csu.edu.cn

† These authors contributed equally to this work.

IntechOpen

References

[1] Gleick PH, Cooley H. Freshwater scarcity. Annual Review of Environment and Resources. 2021;**46**(1):319-348

[2] Salehi M. Global water shortage and potable water safety; Today's concern and tomorrow's crisis. Environment International. 2022;**158**:106936

[3] Kurihara M. Seawater reverse osmosis desalination. Membranes. 2021;**11**(4):243

[4] Ali E, Orfi J, AlAnsary H, Baakeem S, Alsaadi AS, Ghaffour N. Advanced structures of reversal multi-stage flash desalination. Desalination. 2024;**571**:117095

[5] Xu H, Ji X, Wang L, Huang J, Han J, Wang Y. Performance study on a small-scale photovoltaic electrodialysis system for desalination. Renewable Energy. 2020;**154**:1008-1013

[6] Tao P, Ni G, Song C, Shang W, Wu J, Zhu J, et al. Solar-driven interfacial evaporation. Nature Energy. 2018;**3**(12):1031-1041

[7] Kabeel AE, El-Agouz SA. Review of researches and developments on solar stills. Desalination. 2011;**276**(1-3):1-12

[8] Jin H, Lin G, Bai L, Zeiny A, Wen D. Steam generation in a nanoparticle-based solar receiver. Nano Energy. 2016;**28**:397-406

[9] Otanicar TP, Phelan PE, Prasher RS, Rosengarten G, Taylor RA. Nanofluid-based direct absorption solar collector. Journal of Renewable and Sustainable Energy. 2010;**2**(3):033102

[10] Ghasemi H, Ni G, Marconnet AM, Loomis J, Yerci S, Miljkovic N, et al. Solar steam generation by heat localization. Nature Communications. 2014;**5**:4449

[11] Wang Z, Liu Y, Tao P, Shen Q, Yi N, Zhang F, et al. Bio-inspired evaporation through plasmonic film of nanoparticles at the air-water interface. Small. 2014;**10**(16):3234-3239

[12] Wu X, Chen GY, Owens G, Chu D, Xu H. Photothermal materials: A key platform enabling highly efficient water evaporation driven by solar energy. Materials Today Energy. 2019;**12**:277-296

[13] Zhu L, Gao M, Peh CKN, Ho GW. Recent progress in solar-driven interfacial water evaporation: Advanced designs and applications. Nano Energy. 2019;**57**:507-518

[14] Dao V-D, Vu NH, Yun S. Recent advances and challenges for solar-driven water evaporation system toward applications. Nano Energy. 2020;**68**:104324

[15] Zhu L, Gao M, Peh CKN, Ho GW. Solar-driven photothermal nanostructured materials designs and prerequisites for evaporation and catalysis applications. Materials Horizons. 2018;**5**(3):323-343

[16] Kashyap V, Ghasemi H. Solar heat localization: Concept and emerging applications. Journal of Materials Chemistry A. 2020;**8**(15):7035-7065

[17] Chen C, Kuang Y, Hu L. Challenges and opportunities for solar evaporation. Joule. 2019;**3**(3):683-718

[18] Liu H, Huang Z, Liu K, Hu X, Zhou J. Interfacial solar-to-heat conversion for desalination. Advanced Energy Materials. 2019;**9**(21):1900310

[19] Gan Q, Zhang T, Chen R, Wang X, Ye M. Simple, low-dose, durable, and carbon-nanotube-based floating solar still for efficient desalination and purification. ACS Sustainable Chemistry & Engineering. 2019;**7**(4):3925-3932

[20] Gao M, Zhu L, Peh CK, Ho GW. Solar absorber material and system designs for photothermal water vaporization towards clean water and energy production. Energy & Environmental Science. 2019;**12**(3):841-864

[21] Li X, Yao Z, Wang J, Li D, Yu K, Jiang Z. A novel flake-like Cu7S4 solar absorber for high-performance large-scale water evaporation. ACS Applied Energy Materials. 2019;**2**(7):5154-5161

[22] Lin K, Chen R, Zhang L, Shen W, Zang D. Enhancing water evaporation by interfacial silica nanoparticles. Advanced Materials Interfaces. 2019;**6**(16):1900369

[23] Qiblawey HM, Banat F. Solar thermal desalination technologies. Desalination. 2008;**220**(1-3):633-644

[24] Vélez-Cordero JR, Hernández-Cordero J. Heat generation and conduction in PDMS-carbon nanoparticle membranes irradiated with optical fibers. International Journal of Thermal Sciences. 2015;**96**:12-22

[25] Yang J, Pang Y, Huang W, Shaw SK, Schiffbauer J, Pillers MA, et al. Functionalized graphene enables highly efficient solar thermal steam generation. ACS Nano. 2017;**11**(6):5510-5518

[26] Kim K, Yu S, An C, Kim S-W, Jang J-H. Mesoporous three-dimensional graphene networks for highly efficient solar desalination under 1 sun illumination. ACS Applied Materials & Interfaces. 2018;**10**(18):15602-15608

[27] Liu M, Zhang S, Yuan T, Bao C. Low-cost, scalable, and durable coal-based composite aerogel beads solar evaporator for efficient seawater desalination and wastewater purification. Desalination. 2023;**550**:116401

[28] Meng F, Zhang Y, Zhang S, Ju B, Tang B. Rational design of biomass-derived composite aerogels for solar-driven seawater desalination and sewage treatment. Industrial & Engineering Chemistry Research. 2022;**61**(27):9763-9773

[29] Ma X, Tian N, Wang G, Wang W, Miao J, Fan T. Biomimetic vertically aligned aerogel with synergistic photothermal effect enables efficient solar-driven desalination. Desalination. 2023;**550**:116397

[30] Wang Y, Li W, Wei Y, Chen Q. Recyclable monolithic Vitrimer foam for high-efficiency solar-driven interfacial evaporation. ACS Applied Materials & Interfaces. 2023;**15**(11):14379-14387

[31] Liu K, Zhang W, Cheng H, Luo L, Wang B, Mao Z, et al. A nature-inspired monolithic integrated cellulose aerogel-based evaporator for efficient solar desalination. ACS Applied Materials & Interfaces. 2021;**13**(8):10612-10622

[32] Zhang W, Zhang G, Ji Q, Liu H, Liu R, Qu J. Capillary-flow-optimized heat localization induced by an air-enclosed three-dimensional hierarchical network for elevated solar evaporation. ACS Applied Materials & Interfaces. 2019;**11**(10):9974-9983

[33] Li Z, Zhang J, Zang S, Yang C, Liu Y, Jing F, et al. Engineering controllable water transport of biosafety cuttlefish juice solar absorber toward remarkably enhanced solar-driven gas-liquid interfacial evaporation. Nano Energy. 2020;**73**:104834

[34] Song L, Zhang X-F, Wang Z, Zheng T, Yao J. Fe_3O_4/polyvinyl alcohol decorated delignified wood evaporator for continuous solar steam generation. Desalination. 2021;**507**:115024

[35] Ding D, Huang W, Song C, Yan M, Guo C, Liu S. Non-stoichiometric MoO_{3-x} quantum dots as a light-harvesting material for interfacial water evaporation. Chemical Communications. 2017;**53**(50):6744-6747

[36] Chen R, Wu Z, Zhang T, Yu T, Ye M. Magnetically recyclable self-assembled thin films for highly efficient water evaporation by interfacial solar heating. RSC Advances. 2017;**7**(32):19849-19855

[37] Shi Y, Li R, Jin Y, Zhuo S, Shi L, Chang J, et al. A 3D Photothermal structure toward improved energy efficiency in solar steam generation. Joule. 2018;**2**(6):1171-1186

[38] Ye M, Jia J, Wu Z, Qian C, Chen R, O'Brien PG, et al. Synthesis of black TiOx nanoparticles by Mg reduction of TiO_2 nanocrystals and their application for solar water evaporation. Advanced Energy Materials. 2016;**7**(4):1601811

[39] Chen X, Liu L, Yu PY, Mao SS. Increasing solar absorption for Photocatalysis with black hydrogenated titanium dioxide nanocrystals. Science. 2011;**331**(6018):746-750

[40] Wang Y, Ma H, Yu J, Li J, Xu N, Zhu J, et al. All-dielectric insulated 3D Plasmonic nanoparticles for enhanced self-floating solar evaporation under one Sun. Advanced Optical Materials. 2023;**11**(7):2201907

[41] Chen M, He Y, Huang J, Zhu J. Synthesis and solar photo-thermal conversion of Au, Ag, and Au-Ag blended plasmonic nanoparticles. Energy Conversion and Management. 2016;**127**:293-300

[42] Chen S, Sun Z, Xiang W, Shen C, Wang Z, Jia X, et al. Plasmonic wooden flower for highly efficient solar vapor generation. Nano Energy. 2020;**76**:104998

[43] Sun W, Zhong G, Kübel C, Ali FM, Qian C, Wang L, et al. Size-tunable photothermal germanium nanocrystals. Angewandte Chemie International Edition. 2017;**56**(22):6329-6334

[44] de Aberasturi DJ, Serrano-Montes AB, Liz-Marzán LM. Modern applications of plasmonic nanoparticles: From energy to health. Advanced Optical Materials. 2015;**3**(5):602-617

[45] Webb JA, Bardhan R. Emerging advances in nanomedicine with engineered gold nanostructures. Nanoscale. 2014;**6**(5):2502

[46] Zhou L, Tan Y, Ji D, et al. Self-assembly of highly efficient, broadband plasmonic absorbers for solar steam generation. Science Advances. 2016;**2**(4):e1501227

[47] Li T, Liu H, Zhao X, Chen G, Dai J, Pastel G, et al. Scalable and highly efficient mesoporous wood-based solar steam generation device: Localized heat, rapid water transport. Advanced Functional Materials. 2018;**28**(16):1707134

[48] Zhang X-F, Wang Z, Song L, Feng Y, Yao J. Chinese ink enabled wood evaporator for continuous water desalination. Desalination. 2020;**496**:114727

[49] Li L, He N, Yang S, Zhang Q, Zhang H, Wang B, et al. Strong tough hydrogel solar evaporator with wood skeleton construction enabling ultra-durable brine desalination. EcoMat. 2022;**5**(1):e12280

[50] Li Y, Li Q, Qiu Y, Feng H. High-efficiency wood-based evaporators for solar-driven interfacial evaporation. Solar Energy. 2022;**244**:322-330

[51] Traver E, Karaballi RA, Monfared YE, Daurie H, Gagnon GA, Dasog M. TiN, ZrN, and HfN nanoparticles on nanoporous aluminum oxide membranes for solar-driven water evaporation and desalination. ACS Applied Nano Materials. 2020;**3**(3):2787-2794

[52] Li J, Wang X, Lin Z, Xu N, Li X, Liang J, et al. Over 10 kg m^{-2} h^{-1} evaporation rate enabled by a 3D interconnected porous carbon foam. Joule. 2020;**4**(4):928-937

[53] Li X, Xu W, Tang M, Zhou L, Zhu B, Zhu S, et al. Graphene oxide-based efficient and scalable solar desalination under one sun with a confined 2D water path. Proceedings of the National Academy of Sciences. 2016;**113**(49):13953-13958

[54] Li X, Lin R, Ni G, Xu N, Hu X, Zhu B, et al. Three-dimensional artificial transpiration for efficient solar waste-water treatment. National Science Review. 2018;**5**(1):70-77

[55] Xu N, Hu X, Xu W, Li X, Zhou L, Zhu S, et al. Mushrooms as efficient solar steam-generation devices. Advanced Materials. 2017;**29**(28):1606762

[56] Xue G, Liu K, Chen Q, Yang P, Li J, Ding T, et al. Robust and low-cost flame-treated wood for high-performance solar steam generation. ACS Applied Materials & Interfaces. 2017;**9**(17):15052-15057

[57] Zhang H, Li L, Jiang B, Zhang Q, Ma J, Tang D, et al. Highly thermally insulated and superhydrophilic corn straw for efficient solar vapor generation. ACS Applied Materials & Interfaces. 2020;**12**(14):16503-16511

[58] Liu Y, Liu Z, Huang Q, Liang X, Zhou X, Fu H, et al. A high-absorption and self-driven salt-resistant black gold nanoparticle-deposited sponge for highly efficient, salt-free, and long-term durable solar desalination. Journal of Materials Chemistry A. 2019;**7**(6):2581-2588

[59] Xu K, Wang C, Li Z, Wu S, Wang J. Salt mitigation strategies of solar-driven interfacial desalination. Advanced Functional Materials. 2020;**31**(8):2007855

[60] Ren H, Tang M, Guan B, Wang K, Yang J, Wang F, et al. Hierarchical graphene foam for efficient omnidirectional solar–thermal energy conversion. Advanced Materials. 2017;**29**(38):1702590

[61] Sheng M, Yang Y, Bin X, Zhao S, Pan C, Nawaz F, et al. Recent advanced self-propelling salt-blocking technologies for passive solar-driven interfacial evaporation desalination systems. Nano Energy. 2021;**89**:106468

[62] Zhao J, Yang Y, Yang C, Tian Y, Han Y, Liu J, et al. A hydrophobic surface enabled salt-blocking 2D Ti3C2MXene membrane for efficient and stable solar desalination. Journal of Materials Chemistry A. 2018;**6**(33):16196-16204

[63] Xu W, Hu X, Zhuang S, Wang Y, Li X, Zhou L, et al. Flexible and salt resistant Janus absorbers by electrospinning for stable and efficient solar desalination. Advanced Energy Materials. 2018;**8**(14):1702884

[64] Yang Y, Zhao H, Yin Z, Zhao J, Yin X, Li N, et al. A general salt-resistant hydrophilic/hydrophobic nanoporous double layer design for efficient

and stable solar water evaporation distillation. Materials Horizons. 2018;**5**(6):1143-1150

[65] Zhao W, Gong H, Song Y, Li B, Xu N, Min X, et al. Hierarchically designed salt-resistant solar evaporator based on Donnan effect for stable and high-performance brine treatment. Advanced Functional Materials. 2021;**31**(23):2100025

[66] Zhang Q, Li L, Jiang B, et al. Flexible and mildew-resistant wood-derived aerogel for stable and efficient solar desalination. ACS Applied Materials & Interfaces. 2020;**12**(25):28179-28187

[67] Kuang Y, Chen C, He S, Hitz EM, Wang Y, Gan W, et al. A high-performance self-regenerating solar evaporator for continuous water desalination. Advanced Materials. 2019;**31**(23):1900498

[68] Fang Q, Li T, Lin H, Jiang R, Liu F. Highly efficient solar steam generation from activated carbon fiber cloth with matching water supply and durable fouling resistance. ACS Applied Energy Materials. 2019;**2**(6):4354-4361

[69] Li Y, Li Q, Qiu Y, Feng H, Deng R. A novel aerogel-based solar evaporator with triple-layered low-tortuosity pore structures for ultra-high salt resistance. Solar RRL. 2024;**8**(18):2400418

[70] Zou M, Zhang Y, Cai Z, Li C, Sun Z, Yu C, et al. 3D printing a biomimetic bridge-arch solar evaporator for eliminating salt accumulation with desalination and agricultural applications. Advanced Materials. 2021;**33**(34):2102443

[71] Zhang Y, Zhang H, Xiong T, Qu H, Koh JJ, Nandakumar DK, et al. Manipulating unidirectional fluid transportation to drive sustainable solar water extraction and brine-drenching induced energy generation. Energy & Environmental Science. 2020;**13**(12):4891-4902

[72] Fu S, Chen Y, Tao Q, Li C, Liu X, He D. Solar-driven interfacial desalination actively adjusted by the electric field. Separation and Purification Technology. 2023;**327**:124987

[73] Xia Y, Li Y, Yuan S, Kang Y, Jian M, Hou Q, et al. A self-rotating solar evaporator for continuous and efficient desalination of hypersaline brine. Journal of Materials Chemistry A. 2020;**8**(32):16212-16217

[74] Bian Y, Ye Z, Zhao G, Tang K, Teng Y, Chen S, et al. Enhanced contactless salt-collecting solar desalination. ACS Applied Materials & Interfaces. 2022;**14**(29):34151-34158

[75] Cooper TA, Zandavi SH, Ni GW, Tsurimaki Y, Huang Y, Boriskina SV, Chen G. Contactless steam generation and superheating under one sun illumination. Nature Communications. 2018;**9**(1):5086

[76] Xia Y, Hou Q, Jubaer H, Li Y, Kang Y, Yuan S, et al. Spatially isolating salt crystallisation from water evaporation for continuous solar steam generation and salt harvesting. Energy & Environmental Science. 2019;**12**(6):1840-1847